Highlights of Spanish Astrophysics XII, Proceedings of the XVI Scientific Meeting of the Spanish Astronomical Society held on July 15 - 19, 2024, in Granada, Spain. M. Manteiga, F. González Galindo, A. Labiano Ortega, M. Martínez González, N. Rea, M. Romero Gómez, A. Ulla Miguel, G. Yepes, C. Rodríguez López, A. Gómez García and C. Dafonte (eds.), 2025

Virialized equation of state and phase transitions in warm and dense matter using Molecular Dynamics.

Barba-González, D.[1], **Albertus, C.**[1] **and Pérez-García, M.A.**[1]

[1] Department of Fundamental Physics and IUFFyM, University of Salamanca, Plaza de la Merced S/N E-37008, Salamanca, Spain

Abstract

We perform microscopic Molecular Dynamics simulations to study the low-density nuclear Equation of State in the one-component plasma (OCP) approximation, relevant for proto-neutron stars (NS) or supernova matter. Using improved Debye interactions between screened ions, including finite-size effects and Ewald sums, we study their effect on the virial expansion coefficients and phase transitions, i.e. solid-liquid and liquid-gas interfaces. Our findings show that a point-like approach is not sufficiently accurate for describing the behavior of thermal properties, such as energy and stress at the transition points. We discuss several tasks needed for the characterization of mechanical and transport properties relevant in astrophysical scenarios such as warm crusts in proto-NS or NS mergers.

1 Introduction

Neutron Stars (NS) are compact, dense astrophysical objects lying at the final stage of the life of massive stars ($\gtrsim 8\mathrm{M}_\odot$). Their very dense interiors span a wide range of densities and temperatures during their evolution. To describe such a complex system one must, generally speaking, use effective degrees of freedom. These include hadrons or even quarks in the inner core and nuclear clusters or ions in the crust. Within the latter, screened interactions become crucial in the electrically neutral matter description, due to the presence and dynamics of electrons in the thermally relaxing lattice in the NS outer layers following the supernova explosion [1].

The outer crust of a NS is a condensed system where protons and neutrons are yet inside nuclei. It ranges in density between $\sim 10^4$ and $\sim 10^{11}$ g/cm^3, and its temperature highly depends on the evolutionary phase of the NS, going as high as $k_BT \sim 30$ MeV in the early, proto-NS, stage. At these densities and temperatures electrons cannot survive inside atomic orbitals, so are stripped off of nuclei and form a degenerate Fermi gas embedding ions that,

at low enough temperatures or high enough densities form a crystal lattice [2]. However, this sea is not static and as electrostatic forces exist between the positive ions and the negative electrons, the latter are arranged in sheaths around nuclei, thus screening the highly repulsive interaction between nuclei themselves.

The crust is populated by neutron-rich nuclei and its composition is usually calculated by minimizing prescribed free energy functionals for selected ranges of density and population species in the one component plasma approximation (OCP) [3]. These approaches are limited, however, when the aim is to understand correlations, structural or dynamical properties of the material in the crust. This information, together with transport [4] and mechanical properties [5, 6], is instead available by microscopic methods such as the one used in this work, i.e. Molecular Dynamics (MD).

In this contribution, we discuss the ability of MD to extract thermodynamical and mechanical properties of low-density NS material centering the discussion into phase transitions in ionic regions of the NS crust. We show the equations governing the interactions and evolution and results from our original code performing simulations in different phases of the material. We characterize the phase transition through jumps in potential energy and pressure, which allow classification of the transition as first-order and discuss next steps in the study of the crust through microscopic simulations.

2 Potential energy in a screened ion plasma

With the aim of obtaining realistic properties from the low-density phase of the NS crust, we use Molecular Dynamics to solve the N-ion individual dynamics using a prescribed interaction potential, see below. We perform simulations using our code USALMD$_{\mathrm{Gauss-Ewald}}$[7], tailored to efficiently follow the ion trajectories in three-dimensional space in the context of fully ionised nuclei immersed in a degenerate electron Fermi sea. They are subject to electrostatic forces exerted to one-another. Specifically, we model those forces within the Debye-Hückel theory potential which for point-like ions is given by

$$\phi_i\left(\vec{r}\right) = \frac{Z_i}{|\vec{r}-\vec{r_i}|} e^{-\frac{|\vec{r}-\vec{r_i}|}{\lambda_e}} \tag{1}$$

In this paradigm where the stellar medium has a degenerate lepton content, the Debye length scale λ_e is not the usual temperature-dependent quantity. Instead, in the Thomas-Fermi approximation the polarizable electron gas produces a screening length which depends on its relativistic Fermi momentum $k_{F,e}$, and it reads: $\lambda_e = \left(k_{F,e}^2 + m_e^2\right)^{-1/2} \sqrt{\frac{\pi}{4\alpha k_{F,e}}}$ with α being the fine-structure constant and m_e the electron mass.

From this starting point, we develop a more sophisticated approach that takes into account the fact that ions are not point-like particles but their charge is distributed in space around their center. Thus the particle-particle potential is not the simplified Yukawa-like in Eq. 1. We obtain its new form from solving Poisson's equation with a screening term and a Gaussian charge distribution with spread a_i (ρ_{Z_i,a_i}(r)) as the source term $\nabla^2\phi_i(\vec{r}) - \phi_i(\vec{r})/\lambda_e^2 = -\rho_{Z_i,a_i}(r)$ with $\rho_{Z_i,a_i}(r) = Z_i \left(\frac{a_i}{\pi}\right)^{\frac{3}{2}} e^{-a_i r^2}$ and $r = |\vec{r} - \vec{r}_i|$.

We include periodic boundary conditions in the L^3 simulation box and the efficient Ewald summation technique to account in our setting for the long-range interactions, especially important in the low-screening limit. It consists of a splitting of the interaction in a short-range part calculated on a particle-per-particle basis, and a long-range part summed in reciprocal k-space, including up to $n_{k,\max}$ reciprocal Cartesian directions into the energy calculation. A dummy parameter dubbed α_{Ewald} is chosen so as to be able to calculate the short-range part only needing the main simulation box under the minimum image convention, while keeping $n_{k,max}$ the lowest possible to ensure computational efficiency. We also include a self-interaction term to avoid accounting for spurious particle charges introduced by the splitting technique.

Our assumption of a cubic simulation box serves as starting point to more ambitious goals, such as calculating elastic properties of the NS crust. For this one needs to perturb the system away from equilibrium and deform the sample to record its response to such deformation via the components of the stress tensor. The shape of the simulation box is codified in the 3×3 matrix H that transforms the particle's position vectors from the cell frame to the laboratory frame, where the properties are recorded. The cell frame is a unitary cube with orthonormal basis set centered in the origin $(0, 0, 0)$. In this way, for the case of a cubic box, the transformation matrix reads $H = \mathrm{diag(L, L, L)}$. Note that for cubic or even parallelepiped boxes H is diagonal, however if external field forces are exerted over the sample it can develop shear deformations and the off-diagonal elements will also be non-zero [6, 8].

When including both model improvements (finite size and Ewald summation), the resulting total potential energy describing the N ion sample is given by $U = U_{\mathrm{short}} + U_{\mathrm{long-range}} - U_{\mathrm{self}}$, with the individual terms reading

$$\begin{aligned} U_{\mathrm{short-range}} =& \frac{1}{2}\sum_{i=1}^{N_I}\sum_{j\neq i=1}^{N_I} 2Z_j \left(\frac{a_j}{\pi}\right)^{\frac{1}{2}} \frac{e^{-a_j r_{ij}^2}}{r_{ij}} \int_0^\infty r' \phi_{\mathrm{short-range,i}}\left(r'\right) e^{-ar'^2} \sinh\left(2a_j r_{ij} r'\right) dr' \\ & - \frac{2\pi}{V}\sum_{i=1}^{N_I}\sum_{j=1}^{N_I} Z_j \int_0^\infty r'^2 \phi_{\mathrm{short-range,i}}\left(r'\right) dr', \end{aligned} \tag{2}$$

$$U_{\mathrm{long-range}} = \frac{1}{2}\sum_{i,j=1}^{N_I}\sum_{\vec{k}\neq 0} \frac{4\pi Z_i Z_j}{V\left(k^2 + \frac{1}{\lambda_e^2}\right)} \times e^{\frac{-k^2}{4}\left(\frac{1}{a_i} + \frac{1}{\alpha_{\mathrm{Ewald}}}\right)} e^{i\vec{k}\left(\vec{r_i} - \vec{r_j}\right)}. \tag{3}$$

$$U_{\mathrm{self}} = 2\pi \sum_{i=1}^{N_I} \left(\frac{a_i}{\pi}\right)^{\frac{3}{2}} Z_i \int_0^\infty r'^2 \phi_{Z_i,\alpha_{\mathrm{Ewald}}}\left(r'\right) e^{-a_i r'^2} dr'. \tag{4}$$

Here V is the volume of the sample, and $\vec{k} = 2\pi H^{-1^t}\vec{n}$ is a reciprocal lattice vector given by the vector of integers $\vec{n}$ perpendicular to the set of planes $\vec{k}$ represents.

The force exerted on an individual ion i is obtained by taking the gradient of the total energy, $\vec{\nabla}_i U$ with respect to that ion's coordinates. Note that the potential energy expressions are also valid for a multi-component sample as they are written in terms of sums over species.

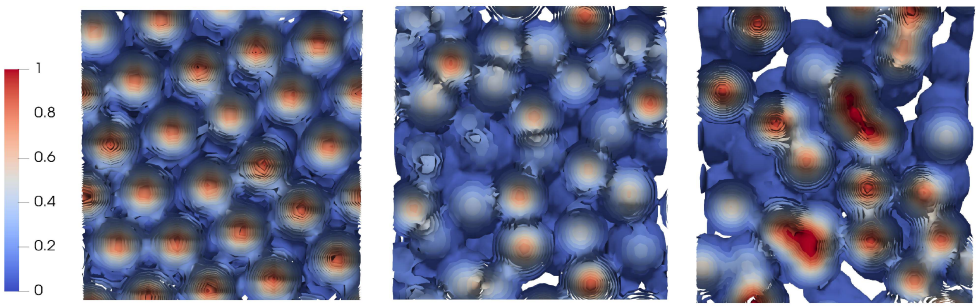

Figure 1: Density isosurfaces (arbitrary scale) for a screened Coulomb OCP of finite-size ion species $(Z, A) = (38, 128)$ at ion density $n_I = 2.06 \times 10^{-6}\,\mathrm{fm}^{-3}$, characteristic of the NS inner-outer crust boundary, as simulated with MD. From left to right, three plasma phases are shown. Left: the plasma is a solid state with T = 0.122 MeV ($\Gamma_C \sim 350$), where lattice order can be clearly seen. Middle: a liquid at T = 0.25 MeV ($\Gamma_C \sim 171$), in which order has been lost due to ion displacement from lattice positions. Right: a gaseous state (T = 10 MeV, $\Gamma_C \sim 4$) where great disorder dominates and high- and low-density regions appear due to ion superposition.

We integrate the dynamical equations in the NVT ensemble while keeping the temperature constant through rescaling particle velocities during evolution. Note that the classical approximation used remains valid as long as their de Broglie wavelengths $\lambda_{dB} = (2\pi/m_i k_B T) \lesssim l$, with $l = (3/4\pi n_I)^{1/3}$ being the average distance between ions.

Thermodynamical properties are extracted from positions and velocities, and averaged over the total number of particles in the ensemble. More concretely, the kinetic energy K is obtained as $K = \sum_i \frac{\vec{p}_i^2}{2m_i}$ while the potential energy U and stress tensor $\Pi_{\alpha\beta}$ $\alpha, \beta = 1, 2, 3$ can be calculated from particle positions. Note that the total pressure is obtained from trace of the stress tensor as $P = \frac{1}{3}\mathrm{Tr}\Pi_{\alpha\beta}$. See [9] for the full set of expressions. In a straightforward way, other thermodynamical potentials of interest are accessible and can be calculated via numerical differentiation, which we have obtained in previous works [7, 9].

3 Solid, liquid, and gas phases in the warm NS crust

One of the main advantages of using MD simulations is their ability to study correlations and scrutinize more realistic features of the material under study. The case of the warm phases in the NS crust is an archetypal example, as it spans a wide range of densities and temperatures. Under such circumstances, the phase diagram of the material can be explored along with the possible phase transitions taking place. The qualitative behavior can thus be captured and analysed through MD, be it via physical magnitudes and their dependence on model parameters or classification into (mainly) first- and second-order phase transitions.

In this work we are dealing with a screened ionic system, electrically neutral, characterized

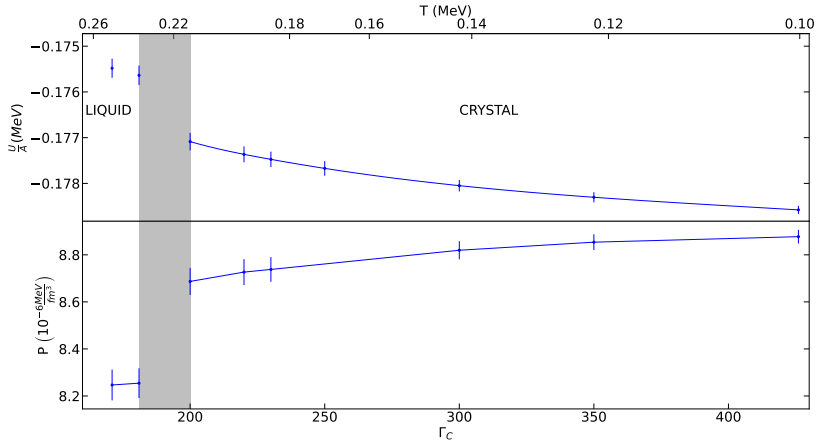

Figure 2: *Top*: Potential energy per baryon as a function of Γ_C and T under Debye potential for both point-like ions and realistic ions interacting through a screened interaction. Composition $(Z, A) = (38, 124)$ and density are typical of the NS outer crust. *Bottom*: Same as top, but for total pressure of the sample. Gray area marks the boundary for the solid-liquid phase transition.

by a single population species embedded in a lepton Fermi sea. One can think of its particular realization in a warm proto-NS crust arising in early cooling stages. In the literature [1], such systems are usually characterized by the point-like Coulomb theory parameter, $\Gamma_C = \frac{Z^2}{lT}$. Γ_C grows with density and decreases with temperature, and its growth represents the system depending less on thermal properties and more on the characteristics of the electrostatic interactions between ions. For a point-like and unscreened interaction, at $\Gamma_C \sim 171.8$ a bcc solid-liquid transition appears [10]. In the more realistic case of screened interaction and finite-sized ions, Γ_C changes and a liquid phase appears at higher values. Thus there is extra dependence, being characterized by additional parameters $\kappa = \frac{l}{\lambda_e}$ and $\eta = \frac{1}{\sqrt{a_i}l}$, respectively for screening and finite size [7, 10]. This occurs because the effect of both $\kappa > 0$ and $\eta > 0$ is to raise the value of potential energy, thus making the system less bound. These two phases are shown as arisen in MD simulations in center (liquid) and left (solid) panels of Fig. 1.

At even lower values of Γ_C one finds a first-order phase transition between liquid and gaseous phases. An example of the latter is depicted in the right panel of Fig. 1 for the studied plasma. The liquid-gas phase transition is expected at $\Gamma_C \sim 10$ [9] with less-known dependences on screening and finite size.

In Fig. 2 we focus on the solid-liquid phase transition, and see how thermodynamical variables, energy per baryon U/A and pressure P, change in the transition region. On the top panel, we show the discontinuity in U/A as a function of temperature and Γ_C, at constant density $n_I = 2.06 \times 10^{-6}\text{fm}^{-3}$, when the phase transition happens at higher than the expected value of ~ 171.8. In the solid phase the system forms a solid bcc lattice, while in the liquid phase it is unordered (fluid). This is due to a combination of finite size and screening, which

as mentioned above, make the system less bound, and easy to melt, driving it into the liquid region of the phase diagram.

We also show the effect on the pressure (bottom panel), calculated from the trace of the stress tensor and displaying a discontinuity at the boundary of the phase transition. It is worth mentioning that both panel discontinuities are finite, which in turn means that the derivatives of potential energy and pressure will show a divergence. In brief, this will allow us to identify the warm OCP screened plasma transition as 1st-order, according to expectations.

4 Conclusions and future work

To summarize, we have shown the capabilities of our state-of-the-art Molecular Dynamics code for warm realistic ionic systems in the NS crust. Allowing for a wide range of temperatures and densities, we have already been able to study in detail many-body complex effects such as crystallization and liquid-gas phase transitions. We have shown the crucial importance of screening and finite size combined in understanding the thermodynamical properties of the crust in the OCP approximation for a neutron-rich heavy species.

Energy expressions shown in Sec. 2 allow not only for static samples, but also ones subject to external forces codified in the deformation matrix. This will allow us to study mechanical properties of the material, such as transport properties and/or its response to deformations through the stress tensor. Further work on these topics is currently in progress.

Acknowledgments

Authors acknowledge partial support from the Spanish Ministry of Science PID2022137887NB-100, RED2022-134411-T, Junta de Castilla y León projects SA101P24, SA091P24 and RES resources under AECT-2024-2-0009 project. D.B.G. acknowledges support from a Ph.D. Fellowship funded by Consejería de Educación de la Junta de Castilla y León and European Social Fund.

References

[1] Chamel, N. & Haensel, P. 2008, Living Rev. Relativity, 11, 10.

[2] Kozhberov, A. A.& Potekhin A. Y. 2021, Phys. Rev. E, 103, 4, 043205

[3] Pearson, J.M., Chamel, N., Potekhin et al, 2018, MNRAS, 481, 2994-3026

[4] Yakovlev, D. G., Kaminker, A. D., Potekhin A. Y. et al. 2021, MNRAS, 500, 4491-4505

[5] Gittins, F., Andersson, N. 2021, MNRAS 507, 116-128.

[6] Caplan, M. E., Schneider, A. S. & Horowitz, C. J. 2018, Phys. Rev. Lett. 121, 132701.

[7] Barba-González, D., Albertus, C., & Pérez-García, M.A. 2022, Phys. Rev. C, 106, 065806.

[8] Horowitz, C. J., Kadau, K 2009, Phys. Rev. Lett. 102, 191102

[9] Barba-González, D., Albertus, C., & Pérez-García, M.A. 2024, MNRAS, 528, 3498-3508.

[10] Khrapak, S. A., & H. M. Thomas 2015, Phys. Rev. E 91, 023108.